The mass of the scalar boson beyond the large-Nc limit

Pallante, E.

Published in:
Zeitschrift für Physik. C: Particles and Fields

DOI:
10.1007/s002880050474

Z. Phys. C 75, 305–313 (1997)

ZEITSCHRIFT
FÜR PHYSIK C

The mass of the scalar boson beyond the large-N_c limit

E. Pallante

NORDITA, Blegdamsvej 17, DK-2100 Copenhagen, Denmark (e-mail: pallante@nbivax.nbi.dk)

Received: 10 June 1996

Abstract. Within the framework of the $1/N_c$ expansion of four-fermion interaction models, we analyse the next to leading $1/N_c$ corrections to the well known large-N_c result $M_S = 2M_Q$ where M_S is the mass of the scalar boson and M_Q is the constituent quark mass. The calculation is performed in the Extended Nambu-Jona Lasinio (ENJL) model which is suitable for describing low energy hadron properties. We treat the model as fully non renormalizable and discuss the comparison with approaches based on the equivalence with renormalizable Yukawa type models. We consider both the $G_V = 0$ and the $G_V \neq 0$ cases with $n_f = 2$ flavours and study the dependence upon the regularization scheme. We find that pure next-to-leading $1/N_c$ corrections are large and negative, while a partially resummed treatment can induce positive and smaller corrections. A triplet-singlet states' splitting is observed.

1 Introduction

The physical content of four-fermion interaction models has been extensively analysed in the past recent years. Within the $1/N$ expansion approach [1] for a general $U(N)$ symmetric model, the equivalence *under certain assumptions* of four-fermion models with scalar four-fermion interactions and Yukawa-type models has been investigated in [2, 3], while the consequences of imposing the so called *compositness condition* have been derived by [4, 5] and most recently by [6]. In all the cases the renormalized ratio of boson and fermion masses plays a relevant role. In [2] is shown that the ratio goes to a fixed value due to the infrared freedom of the renormalizable Yukawa-type model and the assumption that the couplings are generic at the cut-off scale. In addition a common trend of all the analyses seems to be the fact that the large-N_c value of the mass ratio $M_S/M_Q = 2$ gets a large and negative next to leading $1/N_c$ correction for a realistic value $N_c = 3$. This suggests an asymptotic behaviour of the series where each finite order in $1/N_c$ fails to give a good estimate of the real value of the mass ratio for useful values of N_c.

In this paper we address a calculation of the $1/N_c$ next to leading correction to the scalar boson mass based on a treatment of a four-fermion model *à la* Nambu-Jona Lasinio which is alternative to the approaches formulated in [2] and [6] and is of more immediate use in the derivation of hadron properties. In this case the model is treated as fully non renormalizable (see [7] and [8] for reviews).

Effective constituent quark models *à la* Nambu-Jona Lasinio have been found to be successful in reproducing the experimental values of the low-energy coupling constants to $O(p^4)$ in Chiral Perturbation Theory (ChPt) [9]. Here the proper time regularization has been used. Small dependence upon the regularization scheme has been also verified in [10, 7]. Many of the couplings between resonances and pseudoscalar mesons have been computed [9, 11] and nicely compare with the experiment, as well as the vector and axial-vector masses [9, 12].

Large-N_c two and three point functions have been derived in the fully fermionic language via the resummation of linear chains of constituent quark bubbles (sausage diagrams of the Φ^4 theory) [12, 13]. In all the phenomenological results the explicit dependence upon the ultraviolet cut-off of the effective theory is kept treating the model as fully non renormalizable and away from the infrared limit. The large-N_c calculation of the scalar two point function in the fully fermionic language and in the chiral limit reproduces a pole at $M_S = 2M_Q$ [12], where M_Q is the constituent quark mass. With a typical value of $M_Q = 250 \div 350\,\mathrm{MeV}$ one has $M_S = 500 \div 700\,\mathrm{MeV}$. The question arises if this pole has to be identified with a physical hadron state or it remains an artefact of the low energy model possibly related to the lack of confinement. One remote possibility is that the eventual low lying scalar resonance has a very large width.

From the experimental point of view a signal of a narrow scalar state around 750 MeV is reported in [14], while the first clear scalar resonances are the $a_0(983)$ and the isosinglet $f_0(975)$ states. Their interpretation as an ordinary $q\bar{q}$ bound state is dubious [15, 16, 17]. Most recently a fit of the available data [18] indicated that the $K\bar{K}$ component is large for both the $a_0(983)$ and $f_0(975)$ states. It is then clear that the identification of the physical scalar states a_0 and f_0 would probably require the insertion of a mixing with exotic states (glueballs, $K\bar{K}$ bound states etc.) inside a low energy model. This is beyond the scope of this paper.

The present version of the ENJL model only allows for a scalar state which can be elementary or a $\bar{q}q$ composite state. Nonetheless we show that $1/N_c$ corrections to the large-N_c value of the scalar mass can produce a splitting between the octet and the singlet scalar states.

In Sect. 2 we first outline the model and make clear the main differences amongst the present approach and the approaches in [2] and [6] based on the equivalence of the four-fermion interaction models with a renormalizable Yukawa-type model. Then we clarify the correspondence between the non-bosonized version of the ENJL model, where only fermion degrees of freedom are present, and its bosonized version which only contains the auxiliary boson fields once the fermions have been integrated out. The appearance of overlapping divergences in the diagrams which give the $1/N_c$ n.t.l. corrections to the scalar two-point function in the non-bosonized version can prevent from a simple and unambiguous calculation. We chose to compute them in the bosonized version which gives a reliable and fully analytical approximation of the exact result. In Sect. 3 we derive the $1/N_c$ corrections to the scalar pole mass in the $G_V = 0$ case, where only scalar and pseudoscalar meson fields are present in the bosonized action and with $n_f = 2$ flavours. Here a subsection is dedicated to the treatment of leading divergences in this type of theories required by chiral invariance. We also comment on different covariant regularization schemes. In Sect. 4 we extend the model to the case $G_V \neq 0$, where also vector and axial-vector fields are present. For both cases a numerical analysis is shown and the appearance of a mass splitting between the scalar singlet and the non-singlet is obtained. We comment on numerical results and state our conclusions in Sect. 5.

2 Bosonized versus non-bosonized version of the ENJL model

The effective ENJL Lagrangian can be written as follows [9]:

$$\mathscr{L}_{ENJL} = \mathscr{L}^{\Lambda}_{QCD} + \mathscr{L}_{S,P} + \mathscr{L}_{V,A}, \tag{2.1}$$

where $\mathscr{L}_{S,P}$ and $\mathscr{L}_{V,A}$ are all the possible four-fermion lowest dimensional interactions allowed by chiral symmetry and leading in the $1/N_c$ expansion

$$\begin{aligned}\mathscr{L}_{S,P} &= \frac{8\pi^2 G_S(\Lambda)}{N_c \Lambda^2} \sum_{a,b} (\bar{q}^a_R q^b_L)(\bar{q}^b_L q^a_R) \\ &= \frac{4\pi^2 G_S}{N_c \Lambda^2}[(\bar{q}q)^2 - (\bar{q}\gamma_5 q)^2] \\ \mathscr{L}_{V,A} &= -\frac{8\pi^2 G_V(\Lambda)}{N_c \Lambda^2} \sum_{a,b} [(\bar{q}^a_L \gamma_\mu q^b_L)(\bar{q}^b_L \gamma_\mu q^a_L) \\ &\quad +(L \to R)]. \end{aligned} \tag{2.2}$$

At this level the model contains only fermion d.o.f. and is written in terms of three independent parameters: G_S, G_V, and the physical cut-off Λ of the effective interaction. New extra parameters can be hidden in the cut-off procedure which is necessary in a non renormalizable model. The couplings G_S and G_V are explicitly dependent upon the cut-off and we have pulled out a factor $1/N_c$ so that they are $O(1)$ in the $1/N_c$ expansion; a, b are flavour indices and a sum over colour d.o.f is implicit between brackets. $\mathscr{L}^{\Lambda}_{QCD}$ is the QCD Lagrangian in the presence of external sources and in the presence of a low energy cut-off where high frequency quark and gluon modes (i.e. with energy greater than Λ) have been integrated out. The problem of the connection between QCD and this Lagrangian has been addressed in [9]. The non renormalizable (by power counting) part of the Lagrangian (2.1) is in principle the first term of a double expansion in $1/N_c$, where N_c is the number of colours, and in $1/\Lambda^2$.

It is worth at this stage to outline the main differences of our approach with recent analyses of four-fermion models based on their equivalence with renormalizable Yukawa-type models at least in the case $G_V = 0$. There are essentially two pictures explored alternative to the present one. A quite general RG equations analysis of the Gross-Neveu (GN) model has been done by Zinn-Justin in [2] (see also [3] for a numerical study of a NJL model on the same lines), while a NJL model has been studied in [6]. Here the consequences of imposing the *compositness condition* on the scalar field of the renormalizable Yukawa model as an additional constraint are analysed (see also refs. therein).

In the RGE analysis in [2] the mass gap equation and the scalar propagator of the renormalizable generalized GN model in four dimensions reduce to the ordinary GN ones in the infrared limit $\sigma, p \ll \Lambda$, where σ is the vacuum expectation value of the scalar field and p is the typical four-momentum. Then in this case the equivalence of the four-fermion model with the generalized GN model is strictly valid in the *infrared domain* within the $1/N$ expansion. The equivalence can be in principle spoiled beyond the $1/N$ expansion for small values of N. As also pointed out in [2] this regime can be investigated by numerical studies of the four-fermion model in four dimensions and compared with analytic ϵ expansion of the renormalizable model. The type of equivalence in [2] also allows for the presence of higher dimensions operators in the four-fermion model which are irrelevant in $d < 4$ dimensions.

The *compositness condition* on the scalar field of a renormalizable Yukawa model treated in [6] is a stronger extra constraint which guarantees the equivalence between a NJL model and a Yukawa one and which affects the RG flow of the renormalized couplings of the Yukawa model. It spoils the renormalizability of the Yukawa model in four dimensions. One underlying difference between the approaches in [2] and [6] is the fact that the compositness condition implies a particular value of the *bare* couplings at the cut-off scale while they are naturally assumed to be generic in the RG analysis of [2]. The analysis in [6] also provides a prediction for the ratio of the boson and fermion masses at next-to-leading order in the $1/N$ expansion. As will be also true in our case, $1/N$ next-to-leading corrections to the mass ratio are large and negative.

The main difference with our approach is that they keep the original four-fermion model at the infrared limit, which actually corresponds to the limit $\Lambda \to \infty$ or equivalently $\sigma, p \ll \Lambda$. What we do is to keep the model *away from the infrared domain*, which corresponds to being away from the limit $\sigma \ll \Lambda$ in the RGE analysis and in the solution of the mass gap equation. In this case the four-fermion model stays

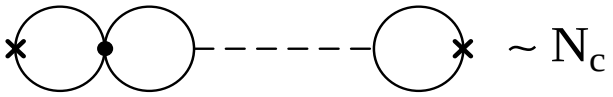

Fig. 1. Two-point function in the non bosonized ENJL model in the large-N_c limit

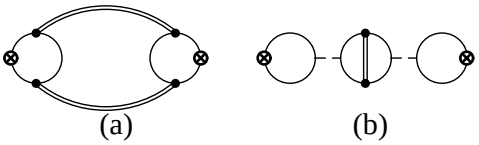

Fig. 2a and b. Two-point function in the non bosonized ENJL model at next-to-leading order in $1/N_c$. Diagrams **a** are self-energy insertions. Diagrams **b** are vertex corrections. The double lines are linear chains of constituent quark bubbles

as non renormalizable and $1/N_c$ corrections to the scalar mass can in principle be derived in the non-bosonized version where only constituent quarks appear.

A full two-point function in the large-N_c limit is given by the infinite resummation of linear chains of quark bubbles with the insertion of a four-quark interaction vertex as shown in Fig. 1. It is of order N_c (each fermion loop gives a factor N_c). Two and three-point functions have been derived in [12, 13]. Analogously a full n-point function in the large-N_c limit is given by the one-constituent quark loop dressed by the insertion of two-point function legs attaching to the external sources.

Next to leading in $1/N_c$ corrections are given in the diagrammatic language by all the possible insertions of one loop of chains of quark bubbles in the large-N_c diagrams. They are of two types: self-energy insertions (Fig. 2a) and vertex corrections (Fig. 2b). Being a non renormalizable model the one loop correction implies a new divergence and thus a new counterterm which we keep the *new* cut-off $\tilde{\Lambda}$ of the loop. The exact calculation of the next to leading in $1/N_c$ corrections to the scalar two-point function (and in particular to its pole mass) involves the one loop insertions of the type 2(a) and 2(b) in the large-N_c scalar two-point function of Fig. 1. Defining the scalar two-point function as $\Pi(q^2) = i\int d^4x\ e^{iqx}\langle 0|TS(x)S(0)|0\rangle$, where $S(x) \equiv -\frac{1}{\sqrt{2}}\bar{q}(x)q(x)$ (we omit for simplicity flavour indices), the large-N_c expression is given by [12]

$$\Pi(Q^2)^{(N_c\to\infty)} = \bar{\Pi}(Q^2)\sum_{n=0}^{\infty}\left(g_S\bar{\Pi}(Q^2)\right)^n = \frac{\bar{\Pi}(Q^2)}{1-g_S\Pi(Q^2)}\,, \tag{2.3}$$

where

$$\bar{\Pi}(Q^2) = \frac{1}{g_S} - (Q^2+(2M_Q)^2)Z_S(Q^2) \tag{2.4}$$

is the bare fermion loop diagram in the mean-field approximation and $Z_S(Q^2)$ is the scalar wave function renormalization constant which in the proper time regularization is given by

$$Z_S(Q^2) = \frac{N_c}{16\pi^2}2\int_0^1 d\alpha\Gamma\left(0,\frac{\alpha(1-\alpha)Q^2+M_Q^2}{\Lambda^2}\right), \tag{2.5}$$

with $\Gamma(0,\epsilon) = \int_\epsilon^\infty dz\frac{1}{z}e^{-z}$ and $g_S = 4\pi^2G_S/N_c\Lambda^2$.

As an example, at next to leading order in $1/N_c$ the resummation of the self-energy insertion diagrams as in Fig. 2a is given by $g_S\Pi = \frac{g_S\bar{\Pi}}{1-g_S\bar{\Pi}} + \frac{1}{1-g_S\bar{\Pi}}g_s\Sigma\frac{1}{1-g_S\bar{\Pi}} + \cdots$ and one gets

$$\Pi(Q^2) = -\frac{1}{g_S}\left(1-\frac{(Z_S(Q^2)g_S)^{-1}}{Q^2+(2M_Q)^2-\Sigma(Q^2)Z_S(Q^2)^{-1}}\right), \tag{2.6}$$

with

$$\Sigma(q^2) = \frac{1}{2}g_S^2\int\frac{d^4k}{(2\pi)^4}\bar{T}(q,k)^2\frac{1}{1-g_S\Pi(k^2)}\,\frac{1}{1-g_S\Pi((q-k)^2)} \tag{2.7}$$

$\bar{T}(q,k)$ is a three-point function vertex of the type SSS, SPP, SVV, SAA, SPA (S=scalar, P=pseudoscalar, V=vector, A=axial-vector).

Because of the appearance of overlapping divergences and the necessity of numerically evaluating contributions like (2.7) due to a complex momenta dependence we chose to estimate them using a reliable and fully analytical approximation within the bosonized version of the model. The correspondence with the non bosonized case is such that a string of quark bubbles is replaced by a meson line with the same quantum numbers. The n.t.l. $1/N_c$ corrections become one loop corrections in the meson theory. In the bosonized version, after integrating over constituent quarks, only the auxiliary boson fields remain: scalar and pseudoscalar in the $G_V = 0$ case and the additional vector and axial-vector fields in the $G_V \neq 0$ case. In what follows we refer to the bosonized version with the non linear realization of the chiral symmetry (i.e. the non linear representation for the pseudoscalar field and derivative coupling of the pseudoscalar to the other degrees of freedom).

Our approximation does correspond in practice to neglecting momenta dependence in vertices and masses of (2.6). We discuss in Sect. 3 the numerical relevance of the approximation. On the more formal side our approximation corresponds to compute the next to leading $1/N_c$ corrections within the bosonized version keeping the leading order contributions in the Heat Kernel Expansion (HKE) approach [9] to the boson vertices and masses. (see also [19] for a review on HKE). Besides this it is easy to verify that the resummed HKE for a given interaction vertex (which is an expansion in powers of ∂^2/M_Q^2) and the large-N_c resummation of quark bubbles produce the SAME momenta dependence.

For the concerns of the numerical evaluation it is useful to notice that the HKE behaves as a slowly convergent series (alternating signs with slowly decreasing coefficients) which implies that the leading term is a better estimate of the exact result than any truncation at a finite order outside the domain $q^2 \ll M_Q^2$. In what follows, only the lowest order in the derivative expansion will be kept for each vertex. This approximation allows us to simplify the calculations and preserves chiral invariance.

3 The $G_V = 0$ case

In the $G_V = 0$ case non renormalizable four-quark interactions in the Lagrangian (2.1) reduce to the scalar and pseu-

doscalar type with one coupling constant G_S. The bosonization introduces scalar and pseudoscalar auxiliary fields and the integration over constituent quarks generates the effective action for the scalar and pseudoscalar physical mesons. The pseudoscalar sector is the ChPt Lagrangian of the pseudo-Goldstone bosons. The effective Lagrangian thus obtained is by construction globally chiral invariant (and locally chiral invariant in presence of external left and right handed sources) and it is non renormalizable being an infinite expansion in powers of derivatives acting on the meson fields. Details on the method can be found in [9].

We restrict ourselves to the $U(2)_L \times U(2)_R$ case (we disregard the effect of the $U(1)_A$ anomaly which is also a next to leading effect in $1/N_c$). The general form of the meson fields, singlets or triplets under $SU(2)_V$, reads

$$M = \sum_{a=1}^{3} \frac{1}{\sqrt{2}} M_{(a)} \tau^{(a)} + \frac{1}{\sqrt{2}} M_0 \mathbf{1}, \tag{3.1}$$

where $\tau^{(a)}, a = 1, ..3$ are the Pauli matrices with $Tr(\tau^a \tau^b) = 2\delta^{ab}$ and M_0 is the singlet component. In the chiral limit ($m_u = m_d = 0$), the effective chiral Lagrangian including scalar and pseudoscalar mesons at leading order $O(p^2)$ in the derivative expansion is given by:

$$\begin{aligned}
\mathscr{L}^{S,P} &= \frac{f_\pi^2}{4} < \xi_\mu \xi^\mu > + \frac{1}{2} < d_\mu S d^\mu S > \\
&\quad - \frac{1}{2} M_S^2 < S^2 > + \mathscr{L}_{int}^{S,P} \\
\mathscr{L}_{int}^{S,P} &= -\frac{\lambda_3}{3!} < S^3 > - \frac{\lambda_4}{4!} < S^4 > + c_d < S \xi_\mu \xi^\mu > \\
&\quad + c_4^{(1)} < S^2 \xi_\mu \xi^\mu > + c_4^{(2)} < S \xi_\mu S \xi^\mu > .
\end{aligned} \tag{3.2}$$

Building blocks of the Lagrangian (3.2) are the scalar field S and the axial current of the pseudoscalar field $\xi_\mu = i\{\xi^\dagger(\partial_\mu - i r_\mu)\xi - \xi(\partial_\mu - i l_\mu)\xi^\dagger\}$, where r_μ and l_μ are the external right-handed and left-handed sources and $\xi = \sqrt{U} = \exp(-\frac{i}{\sqrt{2}}\frac{\Phi}{f_\pi})$ is the usual exponential representation with the pseudoscalar meson matrix Φ defined as in (3.1). Both fields ξ_μ and S transform non linearly under the chiral group $G = U(2)_L \times U(2)_R$ as $\mathscr{O} \to h(\Phi)\mathscr{O}h^\dagger(\Phi)$. The couplings amongst mesons have been derived using the HKE and with proper time regularization. Their expressions are listed in Appendix A. They are functions of the cut-off Λ of the fermion loop, the constituent quark mass M_Q, the axial-pseudoscalar mixing parameter g_A ($g_A = 1$ in the case $G_V = 0$) and the number of colours N_c.

As it is implied by the non renormalizability of the model the values of the parameters are *a priori* regularization dependent. Most suitable regularizations are the covariant ones: proper time, four-momentum cut-off and Pauli-Villars. Explicit solutions of the gap equation of the four-fermion model in the three cases can be found in [7]. A small regularization dependence of the parameters has been found [7, 10].

The next to leading in $1/N_c$ corrections to the pole mass of the scalar two-point function within the bosonized version are given by the one loop corrections to the scalar meson propagator generated by the vertices in (3.2). The diagrams which contribute are the ones in Fig. 3a, the self-energy insertions and 3b, the tadpoles. The diagram 3c does enter the gap equation (it modifies the one point scalar function) and has not to be included in order to avoid double counting. The $1/N_c$ corrections to the gap equation have been considered in [10] and proven to be numerically relevant but still in a perturbative regime. The one boson loops have to be regularized and thus explicitly depend on a *new* cut-off $\tilde{\Lambda}$. This is the signal of the non renormalizability of the model. Physical inputs can be used to constrain its value (see Sect. 3.2). One loop diagrams in Fig. 3 can be up to quartically divergent by naive power counting due to the derivative coupling of the pseudoscalar field. As was noticed in [20] with a specific example of a phenomenological pion Lagrangian à la Weinberg, the quantization of effective theories like the one in (3.2) with an arbitrary number of derivatives, can fail if one uses naive Feynman rules with a cutoff regularization scheme.

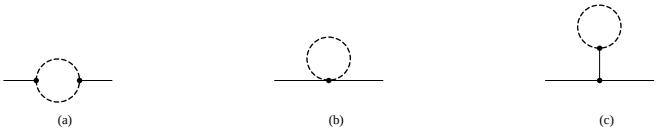

Fig. 3a–c. Two-point scalar function in the bosonized ENJL model at next to leading order in $1/N_c$. Diagrams **a** are self-energy insertions. Diagrams **b** are tadpoles. Diagrams **c** contribute to the one-point scalar function and have to be included in the gap equation

In the next subsection we briefly show that all the leading quartic divergences disappear under the requirement of chiral invariance of the partition function. Our case is a simple extension of the example shown in [20] to an effective theory of pions interacting with scalar fields.

3.1 Quartic divergences versus chiral invariance

The Lagrangian (3.2) satisfies two requisites: a) it is an infinite expansion in powers of derivatives acting on the fundamental fields and b) the fundamental fields transform non linearly under the chiral group. Expanding the field ξ_μ in powers of the Φ field matrix, and reducing covariant derivatives to ordinary ones which enter in our calculation, the Lagrangian (3.2) can be written as $\mathscr{L} = \frac{1}{2} g^{\tilde{a}\tilde{b}}(\Phi, S)\partial_\mu \Phi^{\tilde{a}} \partial^\mu \Phi^{\tilde{b}}$, where $\tilde{a}, \tilde{b}$ are flavour indices going from 0 (for the singlet case) to 3 (for the triplet case) according to the decomposition (3.1). The metric tensor $g^{\tilde{a}\tilde{b}}(\Phi, S)$ is explicitly dependent on the pseudoscalar field and the scalar field due to the presence of interaction terms. We find

$$\begin{aligned}
g^{\tilde{a}\tilde{b}} &= \delta^{\tilde{a}\tilde{b}} \Bigg[1 + \frac{4c_d}{\sqrt{2} f_\pi^2} S_1 \\
&\quad + \frac{2}{f_\pi^2}(c_4^{(1)} + c_4^{(2)}) S_1^2 + \frac{2}{f_\pi^2}(c_4^{(1)} - c_4^{(2)}) \sum_{i=1}^{3} S_i S^i \Bigg] \\
&\quad + (S_a \delta^{0\tilde{b}} + S_b \delta^{0\tilde{a}}) \left(\frac{4c_d}{\sqrt{2} f_\pi^2} + \frac{4}{f_\pi^2}(c_4^{(1)} + c_4^{(2)}) S_1 \right) \\
&\quad + \frac{4}{f_\pi^2} c_4^{(2)} \sum_{i=1}^{3} S_i S^i \delta^{0\tilde{a}} \delta^{0\tilde{b}} + \frac{4}{f_\pi^2} c_4^{(2)} S^a S^b,
\end{aligned} \tag{3.3}$$

with flavour indices a, b=1,...3. The metric tensor $g^{\tilde{a}\tilde{b}}$ defines a non linear chiral transformation of the pseudoscalar field Φ

contained in the original Lagrangian $\mathscr{L} = \frac{1}{2}\delta^{\tilde{a}\tilde{b}}\partial_\mu\Phi^{\tilde{a}}\partial^\mu\Phi^{\tilde{b}}$ with a flat metric $\delta^{\tilde{a}\tilde{b}}$. Under this transformation the full partition function has to be invariant (we are not concerned with anomaly in this context). Since the chiral transformed measure is the original one multiplied by $\delta^4(0)\sqrt{detg^{\tilde{a}\tilde{b}}}$, the chiral invariant partition function is defined in terms of the new Lagrangian $\mathscr{L}' = \mathscr{L} + \delta^4(0)\ln\sqrt{detg^{\tilde{a}\tilde{b}}}$. By doing an expansion in the small couplings to the scalar field we find

$$\ln\sqrt{detg^{\tilde{a}\tilde{b}}} = \frac{8c_d}{\sqrt{2}f_\pi^2}S_1 - \left(\frac{4c_d}{\sqrt{2}f_\pi^2}\right)^2\left(S_1^2 + \frac{1}{2}\sum_{i=1}^{3}S_iS^i\right) + \frac{4}{f_\pi^2}c_4^{(1)}\sum_{i=1}^{3}S_iS^i + \frac{4}{f_\pi^2}(c_4^{(1)}+c_4^{(2)})S_1^2 + O(S^3). \quad (3.4)$$

The new terms with $\delta^4(0) = \int d^4k/(2\pi)^4$ do exactly cancel all the leading quartic divergences generated by diagrams in Fig. 3 whose final expressions are listed in Appendix B. The first term cancels the quartic divergence of Fig. 3c (referred to as "top" diagram in Appendix B) for the pseudoscalar case, the second term cancels the one in Fig. 3a (self-energy) pseudoscalar, and the last two terms the one in Fig. 3b (tadpole) pseudoscalar in the triplet and singlet case respectively.

3.2 Numerical analysis

We have calculated the $1/N_c$ corrections in two cases: 1) assuming that the scalar particle is a singlet and 2) assuming that the quark content of the scalar particle is the same as that of the $\rho(770)$ vector meson. This could be the case of the physical $a_0(983)$ scalar resonance. Obviously our $SU(2)$ calculation has to be interpreted as a first indicative approximation of the fully realistic $SU(3)$ calculation. The self-energy and tadpole contributions are listed in Appendix B for the scalar and pseudoscalar loops and both for the singlet and triplet cases. In the chiral limit ($m_\pi = 0$) all the pseudoscalar one loop corrections vanish. Denoting with $M_S^2 = (2M_Q)^2$ the pole mass of the scalar two-point function in the large-N_c limit, the corrected scalar mass at next-to-leading order in $1/N_c$ with a proper time regularization is the following in the singlet case:

$$\tilde{M}_{S_1}^2 = M_S^2\left[1 + \frac{\lambda_4}{16\pi^2}\Gamma(-1,M_S) - \frac{\lambda_3^2}{16\pi^2}\frac{1}{M_S^2}\Gamma(0,M_S)\right], \quad (3.5)$$

while for the neutral scalar triplet (the one associated with τ_3) we get

$$\tilde{M}_{S_3}^2 = M_S^2\left[1+\frac{2}{3}\frac{\lambda_4}{16\pi^2}\Gamma(-1,M_S) - \frac{1}{2}\frac{\lambda_3^2}{16\pi^2}\frac{1}{M_S^2}\Gamma(0,M_S)\right]. \quad (3.6)$$

Away from the chiral limit (i.e. $m_\pi \neq 0$) the additional corrections we get are as follows:

$$\Delta\tilde{M}_{S_1}^2 = \frac{M_S^2}{16\pi^2}\frac{2m_\pi^2}{f_\pi^2}\left[-\frac{4c_d^2}{f_\pi^2}\left(1-4\frac{m_\pi^2}{M_S^2}\right)\Gamma(-1,m_\pi) - 4(c_4^{(1)}+c_4^{(2)})\frac{m_\pi^2}{M_S^2}\Gamma(-1,m_\pi) + \frac{8c_d^2}{f_\pi^2}\left(1-\frac{m_\pi^2}{M_S^2}\right)\Gamma(0,m_\pi)\right], \quad (3.7)$$

$$\Delta\tilde{M}_{S_3}^2 = \frac{M_S^2}{16\pi^2}\frac{2m_\pi^2}{f_\pi^2}\left[-\frac{2c_d^2}{f_\pi^2}\left(1-4\frac{m_\pi^2}{M_S^2}\right)\Gamma(-1,m_\pi) - 4c_4^{(1)}\frac{m_\pi^2}{M_S^2}\Gamma(-1,m_\pi) + \frac{4c_d^2}{f_\pi^2}\left(1-\frac{m_\pi^2}{M_S^2}\right)\Gamma(0,m_\pi)\right], \quad (3.8)$$

which also include the contribution from the wave function renormalization constant. We notice however that explicit mass terms in the pseudoscalar Lagrangian have not been included. The partial gamma functions $\Gamma(n,M_i)$ of the proper time regularization depend upon the adimensional ratio $M_i^2/\tilde{\Lambda}^2$, with $i = S, P$ and where $\tilde{\Lambda}$ is the *new* cut-off of the one-boson loop. It is worth to notice that the diagrams in Fig. 3c which have not been included here do not generate any mass splitting between the singlet and the triplet scalar component as expected for a contribution to the gap equation, while the self-energy diagrams give to the triplet component half of the contribution to the singlet one.

We have disregarded the splitting between the singlet and the triplet components running in the loops. In the pseudoscalar case this is due to the $U(1)$ axial anomaly, which appears in the effective Lagrangian at next-to-leading order in the $1/N_c$ expansion. In the scalar case it is again a next-to-leading effect in $1/N_c$ as we have shown here, although other sources can compete in this sector like mixing with glueballs.

The numerical evaluation of the $1/N_c$ corrections in (3.5), (3.6), (3.7) and (3.8) needs as input the values of the large-N_c parameters of the ENJL model, Λ and M_Q (or alternatively Λ and G_S) and the *new* one-loop cut-off $\tilde{\Lambda}$. All these quantities are regularization dependent and have to be consistently evaluated in the same scheme. We used the proper time regularization, while the corresponding expressions in the Pauli-Villars scheme can be easily obtained (previous cancellation of the spurious leading divergences due to the non invariance of the measure) through the substitutions listed at the end of Appendix B. For the choice of the numerical value of $\tilde{\Lambda}$ we follow the argument developed in [10] which, although purely phenomenological, provides a self-consistent way of estimating the size of the boson loop cut-off; it proves that keeping the physical value of f_π at n.t.l. order in $1/N_c$ constrains the allowed range for $\tilde{\Lambda}$ to be $\tilde{\Lambda} \leq \tilde{\Lambda}_{max}$, where $\tilde{\Lambda}_{max}$ is of the order of the constituent quark loop cut-off Λ. The values for the large-N_c parameters in the proper time regularization are M_Q = 199 MeV and Λ = 667 MeV in the $G_V = 0$ case (see fit 4 of [8, 9]). The analysis in [7] shows in addition a small dependence of these parameters upon the regularization scheme. In Fig. 4 we show the squared scalar mass corrected at next to leading order in $1/N_c$ and in the chiral limit (formulas

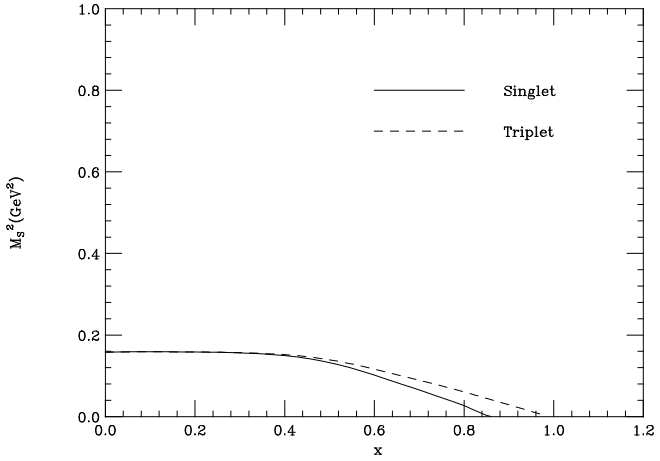

Fig. 4. The squared scalar mass at next-to-leading order in $1/N_c$ in the case G_V = 0 as a function of the ratio $x = \tilde{\Lambda}/\Lambda$ for the singlet case (*solid curve*) and the triplet case (*dashed curve*). Here Λ is fixed at Λ = 667 MeV and M_Q = 199 MeV according to fit 4 of [8]

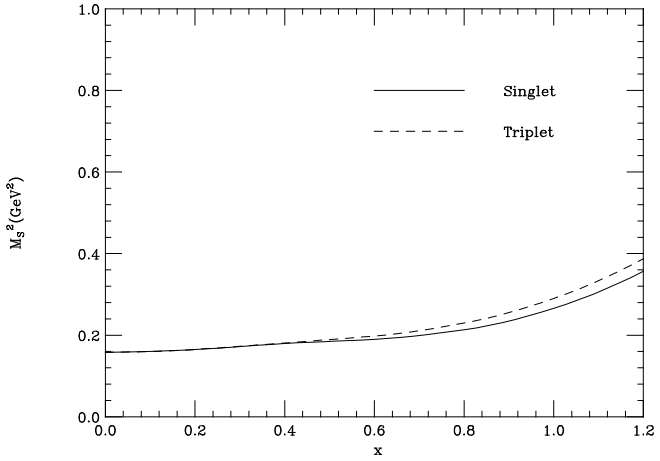

Fig. 5. The partially resummed scalar mass squared using $M_Q(\tilde{\Lambda})$ corrected at next-to-leading order in $1/N_c$ in the case G_V = 0 as a function of the ratio $x = \tilde{\Lambda}/\Lambda$ for the singlet case (*solid curve*) and the triplet case (*dashed curve*). Here Λ is fixed at Λ = 667 MeV and $M_Q(x)$ = 0.199 + .0995x^2 GeV which reproduces a 50% of positive correction to its leading N_c value at x = 1 according to the results in [10]

(3.5) and (3.6)) in the singlet and triplet cases as a function of the boson loop cut-off $\tilde{\Lambda}$ with fixed M_Q = 199 MeV, Λ = 667 MeV. The scalar boson mass M_S^2 in the r.h.s of (3.5) and (3.6) is fixed at its large-N_c value $M_S^2 = 4M_Q^2$. The corrections are negative both to the singlet and the triplet states and push the mass to zero already at $\tilde{\Lambda}/\Lambda \simeq 0.8$. A triplet-singlet splitting is induced which grows with $\tilde{\Lambda}$ but remains small. Away from the chiral limit, with the physical pion mass, pseudoscalar contributions are again negative but suppressed. The behaviour of the genuine next to leading $1/N_c$ corrections seems to be in qualitative agreement with the results based on equivalence arguments as in [2, 6]. The interesting exercise is to take into account the n.t.l. $1/N_c$ corrections to the constituent quark mass M_Q as a solution of the gap equation. This induces a partial resummation of the $1/N_c$ corrections to the scalar boson mass. The $1/N_c$ corrections to the gap equation have been already computed in [10] and they cause a positive shift of the constituent quark mass M_Q as a function of $\tilde{\Lambda}$ for fixed Λ and f_π. In Fig. 5 we show the result of using a running value of $M_Q(\tilde{\Lambda})$ in formulas (3.5) and (3.6)) which qualitatively reproduces the behaviour found in [10]. The surprising result is that the partially resummed corrections are now positive and softer, while the splitting is not modified.

To estimate the error which affects our zero momenta approximation we studied the momentum dependence of each vertex entering the boson loop. All the couplings are weakened by the q^2 corrections and reduced in absolute value by about $20 \div 30\%$ up to $-q^2 \simeq \Lambda^2$. This leads to the conclusion that the q^2 resummed value cannot overcome the approximated value. The same numerical results for the scalar mass in the Pauli-Villars regularization are obtained to a good approximation with the rescaling of the proper-time cut-off $\tilde{\Lambda}_{PT} \simeq 2\sqrt{2}\tilde{\Lambda}_{PV}$.

4 The $G_V \neq 0$ case

The less explored behaviour of four-fermion models is in the presence of vector like interactions, i.e. $G_V \neq 0$ in our case. The Interaction Lagrangian of scalar mesons with vectors and axial-vectors at leading order in the derivative expansion is:

$$\begin{aligned}\mathscr{L}_{int}^{V,A} = & c_V^{(1)} < SV_\mu SV^\mu > + c_V^{(2)} < S^2 V_\mu V^\mu > \\ & + c_{AP} < S\{\xi_\mu, A^\mu\} > + \tilde{c}_A < SA_\mu A^\mu > \\ & + c_A^{(1)} < SA_\mu SA^\mu > + c_A^{(2)} < S^2 A_\mu A^\mu > \ . \end{aligned} \tag{4.1}$$

All the couplings are listed in Appendix A. Notice also the presence at $O(p)$ of the mixed term scalar-pseudoscalar-axial with coupling c_{AP}. The additional diagrams contributing to the scalar pole mass are again the ones in Fig. 3a, b with vector, axial, or mixed axial-pseudoscalar internal lines. All the one loop contributions are listed in Appendix B. In this case quartic divergences can be addressed to two different sources: a) for diagrams with derivative couplings their origin can be the breaking of chiral invariance as for the genuine pseudoscalar case, b) for diagrams with non derivative couplings quartic divergences are a natural consequence of the the bad high energy behaviour of the massive vector propagator $\Delta_{\mu\nu} = (g_{\mu\nu} - k_\mu k_\nu / M_V^2)/(k^2 - M_V^2)$ and they signal the non renormalizability of the massive vector Lagrangian. Divergences of type a) are cancelled following the same demonstration as in 3.1 where the generic field Φ is now replaced by a generic vector field V_μ. They are absent in our case. Divergences of type b) can be cured by the introduction of a spontaneous symmetry breaking mechanism or taking into account the compositness of the vector fields. Nonetheless we observe that a nearly quartic divergence could not be avoided in the calculation within the non bosonized version using the large N_c vector two-point functions predicted in [12], where the running vector mass behaves like $M_V(k) \sim \ln k$. This is the signal of the expected bad high energy behaviour of an effective NJL model. In Appendix B we show the results obtained using the ordinary propagator of a massive vector field $\Delta_{\mu\nu} = (g_{\mu\nu} - k_\mu k_\nu / M_V^2)/(k^2 - M_V^2)$. As an example we also studied the results for the scalar-like propagator with softer renormalizable high energy behaviour

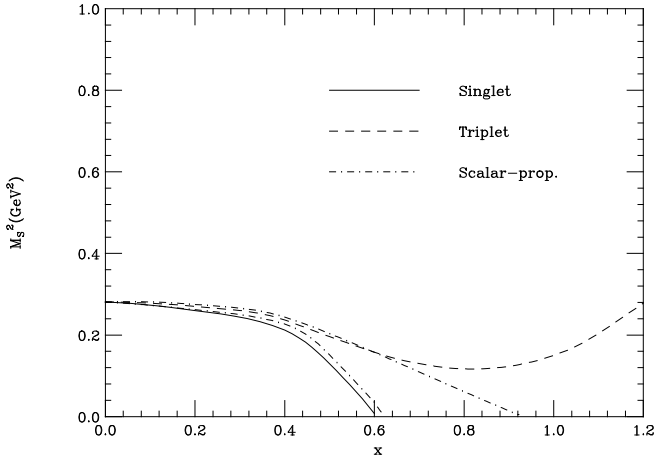

Fig. 6. The squared scalar mass at next-to-leading order in $1/N_c$ in the case $G_V \neq 0$ as a function of the ratio $x = \tilde{\Lambda}/\Lambda$ for the singlet case (*solid curve*) and the triplet case (*dashed curve*). The effect of using the scalar-like vector (axial) propagator is also shown (*dot dashed curve*). Here Λ is fixed at Λ = 1.16 GeV, g_A = 0.61 and M_Q = 265 MeV according to fit 1 of [8]

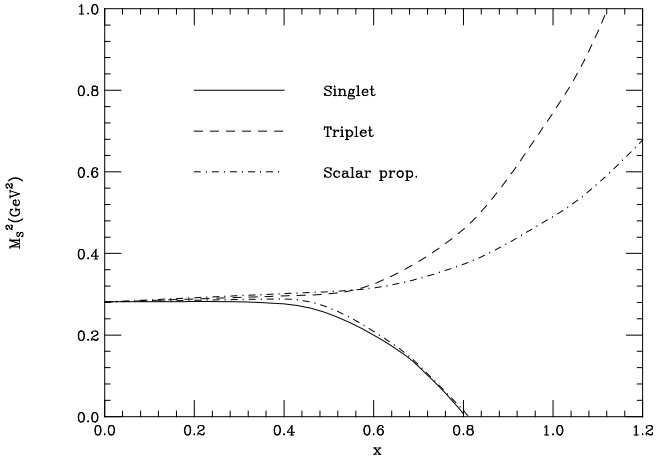

Fig. 7. The squared scalar mass using $M_Q(\tilde{\Lambda})$ corrected at next-to-leading order in $1/N_c$ in the case $G_V \neq 0$ as a function of the ratio $x = \tilde{\Lambda}/\Lambda$ for the singlet case (*solid curve*) and the triplet case (*dashed curve*). The effect of using the scalar-like vector (axial) propagator is also shown (*dot dashed curve*). Here Λ is fixed at Λ = 1.16 GeV g_A = 0.61 and $M_Q(x) = 0.265 + .1325x^2$ GeV which reproduces a 50% of positive correction to its leading N_c value at $x = 1$ according to the results in [10]

$\Delta_{\mu\nu} = g_{\mu\nu}/(k^2 - M_V^2)$. In the chiral limit and for the non renormalizable massive vector (axial) propagator the additional corrections to the scalar mass are as follows:

$$
\begin{aligned}
&\Delta\tilde{M}^2_{S_1} \\
&= \frac{4M_S^2}{16\pi^2}\left\{-\frac{\tilde{c}_A^2}{M_S^2}\left[2\Gamma(-2,M_A)+\left(1+\frac{M_S^2}{2M_A^2}\right)\Gamma(-1,M_A)\right.\right. \\
&+\left(3-\frac{M_S^2}{2M_A^2}\right)\Gamma(0,M_A)\Big] - 2\frac{c_{AP}^2}{f_\pi^2}\frac{M_A^2}{M_S^2}\Big[\Gamma(-2,M_A) \\
&+\left(1-\frac{M_S^2}{2M_A^2}\right)\Gamma(-1,M_A) \\
&+\left(\frac{1}{2}-\frac{M_S^2}{M_A^2}\right)\int_0^1 d\alpha\ \Gamma\left(0,\frac{\alpha M_A^2}{\tilde{\Lambda}^2}\right)\Big] \\
&\left.+(c_A^{(1)}+c_A^{(2)})\frac{M_A^2}{M_S^2}\Big[2\Gamma(-2,M_A)+4\Gamma(-1,M_A)\Big]\right\}, \qquad (4.2)
\end{aligned}
$$

$$
\begin{aligned}
&\Delta\tilde{M}^2_{S_3} \\
&= \frac{4M_S^2}{16\pi^2}\left\{-\frac{1}{2}\frac{\tilde{c}_A^2}{M_S^2}\Big[2\Gamma(-2,M_A)\right. \\
&+\left(1+\frac{M_S^2}{2M_A^2}\right)\Gamma(-1,M_A)+\left(3-\frac{M_S^2}{2M_A^2}\right)\Gamma(0,M_A)\Big] \\
&-\frac{c_{AP}^2}{f_\pi^2}\frac{M_A^2}{M_S^2}\Big[\Gamma(-2,M_A)+\left(1-\frac{M_S^2}{2M_A^2}\right)\Gamma(-1,M_A) \\
&+\left(\frac{1}{2}-\frac{M_S^2}{M_A^2}\right)\int_0^1 d\alpha\ \Gamma\left(0,\frac{\alpha M_A^2}{\tilde{\Lambda}^2}\right)\Big] \\
&+c_A^{(2)}\frac{M_A^2}{M_S^2}\Big[2\Gamma(-2,M_A)+4\Gamma(-1,M_A)\Big] \\
&\left.+c_V^{(2)}\frac{M_V^2}{M_S^2}\Big[2\Gamma(-2,M_V)+4\Gamma(-1,M_V)\Big]\right\}. \qquad (4.3)
\end{aligned}
$$

As in the $G_V = 0$ case, we studied the pure next to leading $1/N_c$ corrected scalar mass and the partially resummed one using for the vector and axial masses M_V = 0.8 GeV and M_A = 1 GeV. The first result is shown in Fig. 6. The large-N_c values of the parameters in the $G_V \neq 0$ case with proper time regularization are M_Q = 265 MeV, Λ = 1.16 GeV and g_A = 0.61 (see fit 1 in [9, 8]). A few comments are in order. The singlet-triplet splitting is enhanced respect to the $G_V = 0$ case. The singlet mass still receives negative corrections. The anomalous enhancement of the triplet mass is sensitively dependent on the form of the propagator. It is consequence of the presence of positive contributions in the vector sector which actually dominate in the case of the ordinary vector propagator form and that are zero in the singlet case. The partially resummed behaviour is shown in Fig. 7. Corrections to the singlet state are softened but still negative. The same anomalous enhancement of the triplet mass is observed. In both cases the singlet-triplet splitting is enhanced respect to the $G_V = 0$ case. Again, on the base of the study of the q^2 dependence of the vector (axial) vertices we expect that the inclusion of the full q^2 dependence will soften the corrections. Within the present approximation the largeness of the axial and vector corrections prevents from a fully reliable estimate in the region $\tilde{\Lambda}/\Lambda \simeq 1$.

5 Conclusions

We studied the next-to-leading in $1/N_c$ corrections to the pole mass of the scalar two-point function within the bosonized version of the Extended NJL model and away from the infrared domain. In this context the model is treated as fully non renormalizable and a new cut-off parameter have to be introduced for the one boson loop. Within a reliable zero momenta approximation, which is the leading order of the Heat Kernel Expansion, we have analytically derived the next-to-leading $1/N_c$ corrections to the scalar mass in both the $G_V = 0$ and $G_V \neq 0$ (vector and axial fields present) cases and studied their regularization scheme dependence. The main results are that genuine next to leading $1/N_c$ corrections to the singlet state are negative and relatively large,

while a partially resummed estimate induces positive and softened corrections in the $G_V = 0$ case. Remarkably the corrections to the large-N_c degenerate mass for the triplet and singlet states induce a splitting which mimics the physical one (octet heavier than the singlet). The splitting effect is enhanced in the $G_V \neq 0$ case.

The largeness of the negative pure next to leading $1/N_c$ corrections derived in this framework qualitatively agrees with the results for the scalar over fermion mass ratio derived in the IR limit where the equivalence with renormalizable Yukawa-type models is valid by the use of the compositness condition [6]. This suggests an asymptotic behaviour of the $1/N_c$ expansion of the mass ratios in four-fermion models both at the IR limit and away from the IR limit, where a truncation at any finite order fails to be a good estimate of the real value for useful values of N_c.

Acknowledgements. I thank Christophe Bruno, who contributed to the early stage of this work. I thank also K. Akama for a kind and useful correspondence on the subject, J. Bijnens for having called my attention to this problem and for many useful discussions, P. Hasenfratz for a stimulating discussion and E. de Rafael for reading the manuscript. The work is supported by the EU Contract Nr. ERBCHBGCT 930442.

A The couplings of the bosonized Lagrangian

The scalar-pseudoscalar couplings are:

$$\begin{aligned}
\frac{\lambda_3}{3!} &= \frac{N_c}{16\pi^2} 4 \frac{M_Q}{Z_S^{3/2}} \left[\Gamma(0,\epsilon) - \frac{2}{3}\Gamma(1,\epsilon) \right] \\
\frac{\lambda_4}{4!} &= \frac{N_c}{16\pi^2} \frac{1}{Z_S^2} \left[\Gamma(0,\epsilon) - 4\Gamma(1,\epsilon) + \frac{4}{3}\Gamma(2,\epsilon) \right] \\
c_d &= \frac{N_c}{16\pi^2} M_Q \frac{2 g_A^2}{\sqrt{Z_S}} \left[\Gamma(0,\epsilon) - \Gamma(1,\epsilon) \right] \\
c_4^{(1)} &= \frac{1}{2} \frac{N_c}{16\pi^2} \frac{g_A^2}{Z_S} \left[\Gamma(0,\epsilon) - \frac{20}{3}\Gamma(1,\epsilon) + \frac{8}{3}\Gamma(2,\epsilon) \right] \\
c_4^{(2)} &= \frac{1}{2} \frac{N_c}{16\pi^2} \frac{g_A^2}{Z_S} \left[\Gamma(0,\epsilon) - \frac{10}{3}\Gamma(1,\epsilon) + \frac{4}{3}\Gamma(2,\epsilon) \right]. \qquad \text{(A.1)}
\end{aligned}$$

The scalar-vector and scalar-axial couplings are:

$$\begin{aligned}
\tilde{c}_A &= \frac{1}{2} \frac{N_c}{16\pi^2} \frac{M_Q}{\sqrt{Z_S} Z_V} \left[4\Gamma(0,\epsilon) - 4\Gamma(1,\epsilon) \right] \\
c_A^{(1)} &= \frac{1}{2} \frac{N_c}{16\pi^2} \frac{1}{Z_S Z_V} \left[\Gamma(0,\epsilon) - \frac{10}{3}\Gamma(1,\epsilon) + \frac{4}{3}\Gamma(2,\epsilon) \right] \\
c_A^{(2)} &= \frac{1}{2} \frac{N_c}{16\pi^2} \frac{1}{Z_S Z_V} \left[\Gamma(0,\epsilon) - \frac{20}{3}\Gamma(1,\epsilon) + \frac{8}{3}\Gamma(2,\epsilon) \right] \\
c_{AP} &= \frac{1}{2} \frac{N_c}{16\pi^2} \frac{g_A M_Q}{\sqrt{Z_S}\sqrt{Z_V}} \left[-4\Gamma(0,\epsilon) + 4\Gamma(1,\epsilon) \right] \\
c_V^{(1)} &= -c_V^{(2)} = \frac{1}{2} \frac{N_c}{16\pi^2} \frac{1}{Z_S Z_V} \left[-\Gamma(0,\epsilon) + \frac{2}{3}\Gamma(1,\epsilon) \right]. \qquad \text{(A.2)}
\end{aligned}$$

All the couplings have been derived within the Heat Kernel Expansion with proper time regularization. Z_V and Z_A are the wave function renormalization constants of the vector and axial-vector fields $Z_V = Z_A = N_c/48\pi^2\Gamma(0,\epsilon)$. The partial gamma functions $\Gamma(n-2,\epsilon)$, with $\epsilon = M_Q^2/\Lambda^2$, are defined as $\Gamma(n-2,\epsilon) = \int_\epsilon^\infty dz 1/z e^{-z} z^{n-2}$. $\Gamma(-2,\epsilon)$ contains a quartic divergence, $\Gamma(-1,\epsilon)$ a quadratic one, $\Gamma(0,\epsilon)$ is logarithmically divergent, while $\Gamma(n,\epsilon)$ with $n > 0$ are finite.

B The one loop contributions

Here the contributions of the three classes of diagrams of Fig. 3 are listed for the scalar (S), pseudoscalar (P), vector (V), axial (A) or mixed axial-pseudoscalar (A-P) bosons running in the loop. They are the self-energy diagrams of Fig. 3a, the tadpole diagrams of Fig. 3b and the top diagrams of Fig. 3c. In the case of axial and vector loops we give the result for the form of the propagator $\Delta_{\mu\nu} = (g_{\mu\nu} - k_\mu k_\nu/M_V^2)/(k^2 - M_V^2)$ and the softer one $\Delta^s_{\mu\nu} = g_{\mu\nu}/(k^2 - M_V^2)$. The self-energy contributions are written in the form $A + Bq^2$ with q^2 Minkowskian and where B gives the wave function renormalization constant which enters the correction to the scalar mass.

Self-energy diagrams

Singlet propagator

$$\begin{aligned}
S &= i \frac{\lambda_3^2}{16\pi^2} \Gamma(0, M_S) \\
P &= i \frac{4 c_d^2}{16\pi^2} \left(\frac{2}{f_\pi^2} \right)^2 \Big[-2 m_\pi^4 \Gamma(-1, m_\pi) \\
&\quad + m_\pi^4 \Gamma(0, m_\pi) + q^2 \Big(\frac{1}{2} m_\pi^2 \Gamma(-1, m_\pi) \\
&\quad - m_\pi^2 \Gamma(0, m_\pi) \Big) \Big] \\
A(\Delta_{\mu\nu}) &= i \frac{4 \tilde{c}_A^2}{16\pi^2} \Big[2\Gamma(-2, M_A) \\
&\quad + \Gamma(-1, M_A) + 3\Gamma(0, M_A) \\
&\quad + \frac{q^2}{2 M_A^2} \Big(\Gamma(-1, M_A) - \Gamma(0, M_A) \Big) \Big] \\
A(\Delta^s_{\mu\nu}) &= i \frac{4 \tilde{c}_A^2}{16\pi^2} \Big[4\Gamma(0, M_A) \Big]
\end{aligned}$$

$$\begin{aligned}
A - P(\Delta_{\mu\nu}) &= i \frac{8 c_{AP}^2}{16\pi^2} \frac{2}{f_\pi^2} \Big[\frac{1}{2} M_A^2 \Gamma(-2, M_A) \\
&\quad + \frac{3}{2} \frac{m_\pi^4}{M_A^2} \Gamma(-2, m_\pi) \\
&\quad + M_A^2 \Big(\frac{1}{2} - \frac{m_\pi^2}{4 M_A^2} \Big) \Gamma(-1, M_A) \\
&\quad - \frac{1}{4} m_\pi^2 \Gamma(-1, m_\pi) - \Big(m_\pi^2 - \frac{(m_\pi^2 + M_A^2)^2}{4 M_A^2} \Big) \\
&\quad \times \int_0^1 d\alpha \; \Gamma\Big(0, \frac{(1-\alpha) m_\pi^2 + \alpha M_A^2}{\tilde{\Lambda}^2} \Big) \\
&\quad + q^2 \Big(-\frac{1}{4} \Gamma(-1, M_A) + \frac{m_\pi^2}{4 M_A^2} \Gamma(-1, m_\pi)
\end{aligned}$$

$$
\begin{aligned}
&-\frac{m_\pi^2+M_A^2}{2M_A^2}\\
&\int_0^1 d\alpha\ \Gamma\left(0,\frac{(1-\alpha)m_\pi^2+\alpha M_A^2}{\tilde{\Lambda}^2}\right)\Bigg)\Bigg]\\
A-P\,(\Delta^s_{\mu\nu}) &= i\frac{8c_{AP}^2}{16\pi^2}\frac{2}{f_\pi^2}\left[M_A^2\Gamma(-1,M_A)\right.\\
&\left.-m_\pi^2\int_0^1 d\alpha\ \Gamma\left(0,\frac{(1-\alpha)m_\pi^2+\alpha M_A^2}{\tilde{\Lambda}^2}\right)\right].
\end{aligned}
\tag{B.1}
$$

Notice that no vertex SVV is allowed.

Triplet propagator

The only possible self-energy diagrams for the triplet propagator contain two different internal lines, one singlet and one triplet. The contribution is half the contribution to the singlet propagator displayed above.

Tadpole diagrams

Singlet propagator

$$
\begin{aligned}
S &= -i\frac{\lambda_4}{16\pi^2}M_S^2\Gamma(-1,M_S),\\
P &= i\frac{4(c_4^{(1)}+c_4^{(2)})}{16\pi^2}\frac{2}{f_\pi^2}m_\pi^4\Gamma(-1,m_\pi)\\
A(V)\,(\Delta_{\mu\nu}) &= -i\frac{4(c_{A(V)}^{(1)}+c_{A(V)}^{(2)})}{16\pi^2}M_{A(V)}^2\\
&\quad\times\left[2\Gamma(-2,M_{A(V)})+4\Gamma(-1,M_{A(V)})\right]\\
A(V)\,(\Delta^s_{\mu\nu}) &= -i\frac{4(c_{A(V)}^{(1)}+c_{A(V)}^{(2)})}{16\pi^2}M_{A(V)}^2\\
&\quad\times\left[4\Gamma(-1,M_{A(V)})\right].
\end{aligned}
\tag{B.2}
$$

Notice that in the singlet case there are no contributions from vector vertices of order $O(p^0)$ like $< S^2V_\mu V^\mu >$, because $c_V^{(1)}+c_V^{(2)}=0$.

Triplet propagator

$$
\begin{aligned}
S &= -i\frac{2}{3}\frac{\lambda_4}{16\pi^2}M_S^2\Gamma(-1,M_S)\\
P &= i\frac{4c_4^{(1)}}{16\pi^2}\frac{2}{f_\pi^2}m_\pi^4\Gamma(-1,m_\pi)\\
A(V)\,(\Delta_{\mu\nu}) &= -i\frac{4c_{A(V)}^{(2)}}{16\pi^2}M_{A(V)}^2\\
&\quad\left[2\Gamma(-2,M_{A(V)})+4\Gamma(-1,M_{A(V)})\right]\\
A(V)\,(\Delta^s_{\mu\nu}) &= -i\frac{4c_{A(V)}^{(2)}}{16\pi^2}M_{A(V)}^2\left[4\Gamma(-1,M_{A(V)})\right]
\end{aligned}
\tag{B.3}
$$

Top diagrams

$$
\begin{aligned}
S &= i\frac{\lambda_3^2}{16\pi^2}\Gamma(-1,M_S)\\
P &= -i\frac{2\lambda_3 c_d}{16\pi^2}\frac{2}{f_\pi^2}\frac{1}{M_S^2}m_\pi^4\Gamma(-1,m_\pi)\\
A\,(\Delta_{\mu\nu}) &= i\frac{2\lambda_3\tilde{c}_A}{16\pi^2}\frac{M_A^2}{M_S^2}\left[2\Gamma(-2,M_A)+4\Gamma(-1,M_A)\right]\\
A\,(\Delta^s_{\mu\nu}) &= i\frac{2\lambda_3\tilde{c}_A}{16\pi^2}\frac{M_A^2}{M_S^2}\left[4\Gamma(-1,M_A)\right].
\end{aligned}
\tag{B.4}
$$

Contributions are the same for singlet and triplet propagator.

Pauli Villars regularization

For the comparison with the proper time regularization contributions the following substitutions can be performed:

$$
\begin{aligned}
m^2\Gamma(-1,m) &\to m^2[(1+2x)\ln(1+2x)\\
&\quad -2(1+x)\ln(1+x)]\\
\Gamma(0,m) &\to 2\ln(1+x)-\ln(1+2x),
\end{aligned}
\tag{B.5}
$$

where $x=\tilde{\Lambda}^2/m^2$. This corresponds to the usual Pauli Villars procedure in a scalar theory where two additional fields with masses $M_1=m+\tilde{\Lambda}$ and $M_2=m+2\tilde{\Lambda}$ and coefficients $C_1=-2$ and $C_2=1$ are sufficient to make the theory finite. In the case of a non linearly realized symmetry (as in this case for the pseudoscalar sector) quartic divergences due to the non invariance of the measure have to be treated before.

References

1. G. t'Hooft, Nucl. Phys. **B 72** (74) 461.
2. J. Zinn-Justin, Nucl. Phys. **B367** (1991) 105;
3. A. Hasenfratz et al., Nucl. Phys. **B365** (91) 79.
4. K. Shyzuya, Phys. Rev. **D** 21 (80) 2327.
5. S. Weinberg, Phys. Rev. 130 (63) 776; D. Lurié and A.J. Macfarlane, Phys. Rev. 136 (64) 816; D. Campbell et al., Phys. Rev. **D** 19 (79) 549.
6. K. Akama, Phys. Rev. Lett. 76 (96) 184.
7. S.P. Klevansky, Rev. Mod. Phys. 64 (92) 656.
8. J. Bijnens, Phys. Rep. 265 (96) 369.
9. J. Bijnens, C. Bruno and E. de Rafael, Nucl. Phys. **B390** (1993) 501.
10. V. Dmitrasinović, H.-J. Schulze and R. Tegen, Ann. of Phys. 238 (95) 332.
11. J. Prades, Z. Phys. **C63** (1994) 491.
12. J. Bijnens, E. de Rafael and H. Zheng, Z. Phys. **C62** (1994) 437.
13. J. Bijnens and J. Prades, Z. Phys. **C64** (1994) 475.
14. M. Svec, Phys. Rev. **D53** (1996) 2343;
    M. Svec et al., Phys. Rev. **D45** (1992) 55, Phys. Rev. **D46** (1992) 949.
15. A. Bramon and E. Massó, Phys. Lett. **93B** (1980) 65;
16. Achasov, Z. Phys. **C41** (1988) 309.
17. J. Weinstein and N. Isgur, Phys. Rev. **D27** (1983) 588.
18. N. Tornqvist, hep-ph 9504372, preprint HU-SEFT R 1995-05.
19. R. Ball, Phys. Rep. 182 (89) 1.
20. J. Honerkamp and K. Meetz, Phys. Rev. **D3** (1971) 1996.